Bull. Mater. Sci., Vol. 29, No. 7, December 2006, pp. 709–716. © Indian Academy of Sciences.

Preparation and characterization of nanostructured CuO thin films for photoelectrochemical splitting of water

DIWAKAR CHAUHAN, V R SATSANGI†, SAHAB DASS and ROHIT SHRIVASTAV*

Department of Chemistry, †Department of Physics and Computer Science, Dayalbagh Educational Institute, Agra 282 005, India

MS received 16 June 2006; revised 7 August 2006

Abstract. Nanostructured copper oxide thin films (CuO) were prepared on conducting glass support (SnO_2: F overlayer) via sol–gel starting from colloidal solution of copper (II) acetate in ethanol. Films were obtained by dip coating under room conditions (temperature, 25–32°C) and were subsequently sintered in air at different temperatures (400–650°C). The evolution of oxide coatings under thermal treatment was studied by glancing incidence X-ray diffraction and scanning electron microscopy. Average particle size, resistivity and band gap energy were also determined. Photoelectrochemical properties of thin films and their suitability for splitting of water were investigated. Study suggests that thin films of CuO sintered at lower temperatures (≈ 400°C) are better for photoconversion than thick films or the films sintered at much higher temperatures. Plausible explanations have been provided.

Keywords. Nanostructured thin film; copper oxide; sol–gel; photoelectrochemical cell; water splitting.

1. Introduction

Copper forms two well known oxides: cuprite (Cu_2O) and tenorite (CuO) (Richthofen *et al* 1997). A metastable copper oxide, paramelaconite (Cu_4O_3), which is an intermediate compound between the previous two, has also been reported (Li *et al* 1991). While Cu_2O forms a cubic structure with a lattice parameter of 4·27 Å, the Cu_4O_3 bears a tetragonal structure having lattice parameters: a = 5·837 Å and c = 0·9932 Å. In CuO, units of CuO_2 are chained and Cu forms four coplanar bonds with oxygen (Ohya *et al* 2000). Amongst the mono oxides of 3*d* transition series elements, CuO is unique as it has a square planar coordination of copper by oxygen in the monoclinic structure. The lattice parameters of CuO are a = 4·684 Å, b = 3·425 Å, c = 5·129 Å and β = 99·28° (Lanke and Vedawyas 1999).

CuO is attractive as a selective solar absorber since it has high solar absorbency and a low thermal emittance (Yoon *et al* 2000). Furthermore, it is a promising semiconductor for solar cell fabrication due to its suitable optical properties (Oral *et al* 2004). It also possesses an incommensurate antiferromagnetic structure below the Neel temperature of 230 K, which is quite unusual (Eliseev *et al* 2000). In some recent reports, CuO has shown high temperature superconductivity as well, where the specific coordination between Cu and O atoms play a crucial role (Ray *et al* 2001). Due to the existence of copper vacancies in the structure, CuO exhibits native *p*-type conductivity (Jeong and Choi 1996). The tentative energy band diagram of CuO is shown in figure 1. Its band gap is reported to be between 1·3 and 1·7 eV with a black colour and a partial transparency in the visible range (Ohya *et al* 2000). Its valence band is reported to lie at 5·42 eV below the vacuum level and is made up mainly from Cu^{2+}–3*d* wave functions. Similarly the conduction band reportedly lies at 4·07 eV below vacuum level. An oxygen –2P type band is also present at 7·33 eV below vacuum level (Koffyberg and Benko 1982). CuO is readily available and nontoxic and this makes it even more attractive for different applications (Oral *et al* 2004).

Research on photoelectrochemical (PEC) cells, particularly their use in solar energy conversion, has gained importance in the last few decades (Chandra Babu *et al* 1994). PEC cells convert solar energy into storable chemical energy as hydrogen through the photoelectrolysis of water. A semiconductor, to be used as photoelectrode in PEC cell, must be chemically stable and should have an optimum band gap (≈ 1·8 eV) so that it may efficiently absorb bulk of solar radiations (Agrawal *et al* 2003). Semiconductors such as TiO_2 (Yoko *et al* 1991), $SrTiO_3$ (Salvador *et al* 1984), SnO_2 (Yoon and Chung 1992) and $BaTiO_3$ (Stilwell and Park 1982) have been investigated as alternative photoelectrodes. But, due to relatively high band gap, they cannot absorb large portion of visible light. On the other hand, low band gap materials viz. Si (Levy-Clement *et al* 1991), GaAs (Fan and Bard 1980)

*Author for correspondence (rohitshrivastav_dei@yahoo.co.in)

and InP (Chandra *et al* 1985) get easily corroded on coming into contact with the electrolyte.

Nanostructured materials, in contrast to their bulk counterparts, exhibit significant alteration in their properties, viz. band gap, porosity and surface area, which are crucial for PEC applications (Armelao *et al* 2003; Morales *et al* 2005). Besides, alteration in above properties are particle size dependent to the extent that even a small change in particle/grain size may generate a material with drastically different characteristics (Chaudhary *et al* 2004). The idea of exploiting nanomaterials to achieve efficient PEC splitting of water has been coined recently (Chaudhary *et al* 2004). Nanostructured CuO is one of the potential materials for this purpose but not many reports exist, so far, exploring this aspect (Yoon *et al* 2000; Chaudhary *et al* 2004). This report deals with the preparation of thin films of nanostructured CuO by sol–gel dip coating, their structural and optical characterization and investigation on their possible role in PEC splitting of water.

2. Experimental

2.1 *Preparation of thin films of copper oxide*

The starting compound used in this study was copper (II) acetate. The choice was made taking into account the fact that hydrolysis of acetate group gives products which are soluble in the solvent medium and get easily decomposed into volatile compounds under heat treatment (Armelao *et al* 2003). A colloidal solution of copper acetate in ethanol was used as precursor. Copper acetate added to ethanol (10 g dm^{-3}) was stirred for 1 h. The resulting solution was sonicated for 2 h, kept overnight for stabilization and used to deposit film. Films were obtained by dip-coating, a process comprising repeated withdrawal of substrate from fluid sol by gravitational draining of sol. The solvent evaporation, accompanied by further condensation reactions, resulted in deposition of a solid film onto the substrate. When compared to conventional thin film forming processes such as chemical vapour deposition, evaporation, or sputtering, the sol–gel dip coating requires considerably less equipment and is potentially less expensive. Besides, in this method the microstructure of the deposited film can be easily tailored by regulating the preparation conditions, viz. solution concentration, annealing temperature and annealing environment (Oral *et al* 2004). TCO glass plates (having SnO_2: F overlayer on one side) were used as substrate, which were washed before film deposition by soaking (for 2–5 min) in the following solvents in the same order: HCl, double distilled water, HF, double distilled water, acetone, double distilled water. Cleaned substrates (3×2 cm) were dried in an oven at 40°C and stored in moisture and dust-free environment by placing inside an air-tight glass container. Films were deposited at room temperature by first hanging vertically (length wise) TCO plates over the copper acetate precursor solution so that nearly 3/4th length of plates is dipped. The plates were, subsequently, slowly withdrawn by gravitational draining of the solution at a speed of ~ 5 cm min^{-1}. By using multi-dipping process, without any thermal treatment between successive layers, replicate samples were obtained which were sintered at 400, 450, 500, 550, 600 and 650°C for 1 h in muffle furnace, in air. Before sintering, film deposited on nonconducting side/surface of TCO plates was removed by mechanical scratching. The sintered film samples appeared black, homogeneous, well adherent to the substrate and were free from cracks and pinholes.

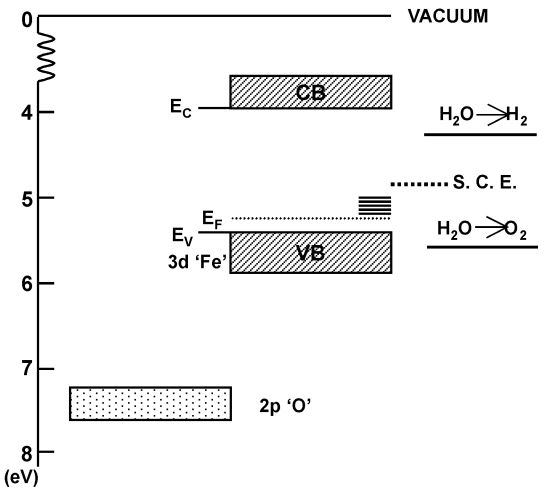

Figure 1. Energy band diagram of CuO.

2.2 *PEC study*

Films were used as working electrodes (WE) in PEC cells. To develop WE an ohmic electrical contact was created from one edge of the substrate (where film was not deposited) with silver paint and a copper wire. Excluding an area of 2·25 cm^2 (1·5 × 1·5 cm) at the centre of the film, all edges and the electrical contact were sealed by a non-transparent, non-conducting epoxy resin, hysol (Dexter, Singapore). PEC studies were conducted using three-electrode configuration electrochemical cell, which had a pyrex window for incoming radiations, and a water jacket, around it, to prevent heating effects. The semiconductor, WE, was used in association with a platinum foil counter electrode (CE) and saturated calomel reference electrode (SCE). Aqueous solution of NaOH (pH = 13), was used as electrolyte and this solution was purged with N_2 for 15–20 min just before PEC study. A Potentiostat (Model ECDA-001, Conserv Enterprises) and 150 W Xenon Arc lamp (Oriel, USA, used as light source) were employed to record current–voltage (*I–V*) characteristics of the cell, both under darkness and illumination. The variation in capacitance with applied bias voltage was also recorded and the

data was utilized to evaluate the values of flat band potential and charge carrier density.

Reagents with purity > 99·9% and double distilled deionized water (specific conductance < 10^{-6} mho cm^{-1}) were used throughout the study. Film samples were prepared in triplicate and with each sample 3–5 repetitive measurements were recorded.

3. Results and discussion

Data presented in table 1 clearly indicate significant rise in resistivity of copper oxide films with increase in sintering temperature, providing the least resistant films at lowest sintering temperature, i.e. 400°C. Film thickness increases with increase in number of layers. Besides, the film thickness added per layer of coating also increases with increase in number of layers. Resistivity depends upon film thickness as well, and is slightly higher for thicker films. Measured density of films ranged from 2·16–2·56 g cm^{-3} which is ≈ 38–45% of theoretical density of CuO. This suggests that the films are porous and can provide a larger contact area with electrolyte when used in PEC cell.

Thin films of copper oxide were subjected to phase analysis by employing X-ray diffractometer (Philips, Model: X'PERT PW3020), that was equipped with graphite monochromator, a mirror at a fixed incidence angle of 1·5° and CuKα-1 as radiation source (λ = 1·54184 Å). The angular accuracy was 0·001° and the angular resolution was better than 0·01°. Figure 2 shows glancing angle X-ray diffraction patterns of copper oxide films obtained at different sintering temperatures and reveal formation of single phase CuO with tenorite structure. The peaks at 2θ angle 35·57, 38·76, 61·60, 65·88 and 67·99° with d_{hkl} 2·5, 2·3, 1·5, 1·4 and 1·4 Å correspond to diffraction from planes ($\bar{1}11$), (111), ($\bar{1}13$), (022) and (113), respectively, of CuO. The lattice parameters of films were calculated as a = 4·67–4·72 Å, b = 3·42–3·49 Å, c = 5·12–5·20 Å and β = 99·20–99·60°, which are very close to the expected values from JCPDS 05-0661, for CuO. The exclusive formation of CuO (tenorite) in sol–gel derived copper oxide films, sintered in air at 100–900°C, was reported even earlier and the present study reconfirms this fact. But, this observation is in contrast to the report of Yoon *et al* (2000), where they have indicated that at temperatures above 300°C, CuO (tenorite) is unstable and is converted to Cu_2O (cuprite). These contradictory reports, probably, suggest that a complex microstructural evolution occurs under annealing in copper oxide films, which is guided by several inter-related and obscure parameters. Further, the presence of multiple peaks of the CuO phase indicates the polycrystalline nature of films (Maruyama 1998). In earlier studies, CuO films obtained by ion beam sputtering and chemical vapour deposition were also reported to be polycrystalline (Maruyama 1998; Yoon *et al* 2000). Relative intensities of the peaks in XRD pattern suggest that there is no grain orientation in the samples (Oral *et al* 2004). With the increase in sintering temperature of film from 400–600°C, the crystalline character of CuO increases as is indicated by rise in intensity of peaks (Armelao *et al* 2003). However, when sintering temperature is raised further to 650°C, there appears to be a slight decrease in crystallinity.

Table 1. Measured resistivity and thickness of copper oxide films.

Sintering temperature (°C)	Number of layers	Thickness* (μm) Mean ± S.D.	Resistivity* (Ω cm) Mean ± S.D.
400	10	4·13 ± 0·06	127 ± 4
450	10	4·12 ± 0·04	131 ± 5
500	10	3·91 ± 0·04	134 ± 5
550	10	3·71 ± 0·04	160 ± 6
600	10	3·70 ± 0·03	231 ± 8
650	10	3·62 ± 0·04	371 ± 11
450	6	0·48 ± 0·04	120 ± 4
450	8	2·61 ± 0·05	129 ± 4
450	12	4·99 ± 0·07	133 ± 6

*Values represent a mean of 10–15 observations; S.D.: standard deviation.

Utilizing the X-ray diffraction data and Scherrer's equation (1), the average particle/grain size in CuO films was computed (Klug and Alexander 1974)

$$B = 0{\cdot}9\lambda/t\cos\theta, \quad (1)$$

where t is grain size, B the full width at half maxima and λ the wavelength of X-ray used (1·54814 Å). The computed values are presented in table 2.

Scanning electron microscope (SEM) (Model: JEOL JSMS 800LV) was used to examine the surface morphology of CuO films and the results are shown in figure 3. In general, films are homogeneous and continuous. Separate coating layers are not visible in sintered films. There seems to be a mismatch in average size of grains/particles determined through Scherrer's calculation utilizing XRD data and SEM analysis. SEM images suggest size of grains to be much larger. Further, while Scherrer's calculation suggests an increase in particle size with rise in sintering temperature, SEM images indicate almost a reverse trend. Taking into account the above discrepancy and the fact that SEM analysis reveals formation of particles with different shapes and sizes, it seems appropriate to consider that the particles which appear in SEM images are, in fact, grain agglomerates, which get fragmented with rise in sintering temperature. In films sintered at 400, 450 and 500°C, relatively larger particles/grain agglomerates can be seen compared to films sintered at higher temperatures. In films sintered at 550°C, the film morphology appeared most uniform and the particle size also lowest. With further rise in sintering temperature, it seems that there occurs some fusion of grain boundaries resulting in a marginal

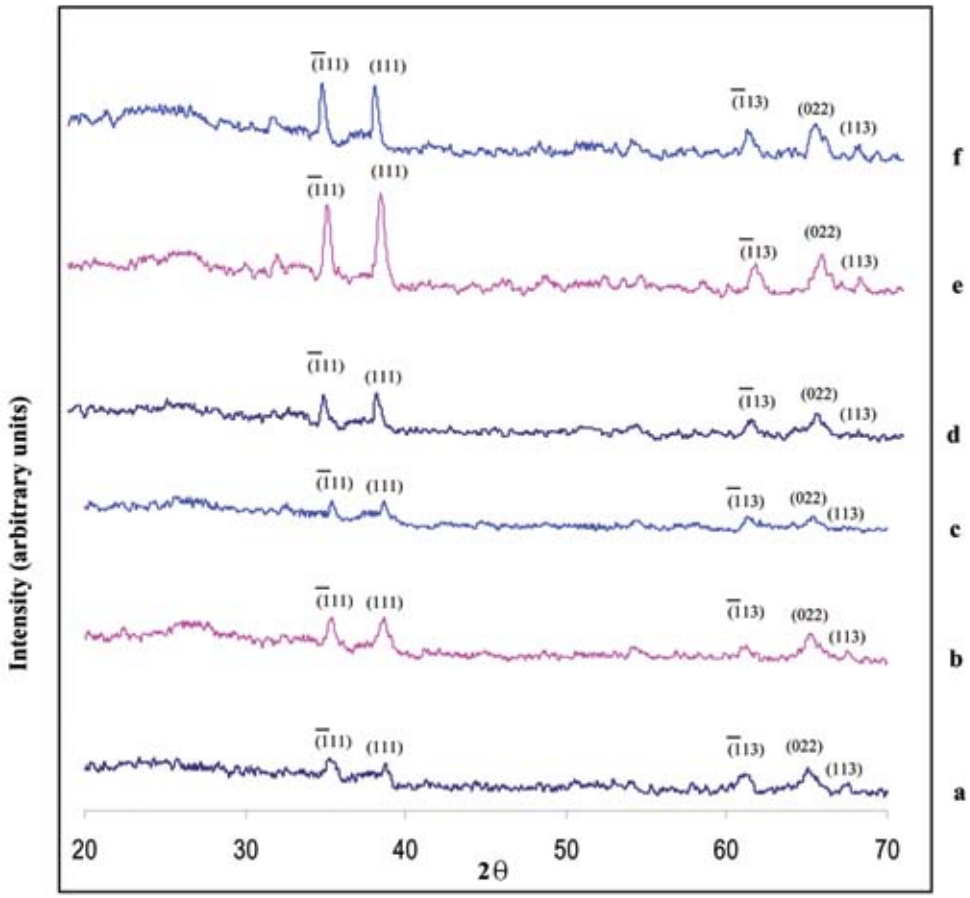

Figure 2. X-ray diffraction pattern of ten layered copper oxide films sintered at: (a) 400, (b) 450, (c) 500, (d) 550, (e) 600 and (f) 650°C.

Table 2. Average size of particles/grains in copper oxide film and its variation with sintering temperature.

Sintering temperature (°C)	Particle size from Scherrer's calculation* (nm) Mean ± S.D.	Particle size from SEM analysis (μm)
400	20 ± 4	8·13
450	30 ± 7	7·65
500	35 ± 6	2·81
550	69 ± 7	0·59
600	81 ± 9	0·62
650	90 ± 9	0·63

*and S.D.: same as in table 1.

increase in particle size. Richthofen *et al* (1997) had reported columnar growth in films of copper oxide. But no such grain elongation in a preferred direction is seen here. The random distribution of grains, in projection and size, only suggests a random nucleation mechanism, and random orientation of grains show that the grain growth is isotropic (Oral *et al* 2004).

The UV-*vis* photospectra of CuO thin films were recorded with respect to the bare substrate placed in the reference beam using double beam spectrophotometer (Shimadzu, Model: UV-2450) in the range 400–800 nm (figure 4). The spectra were analysed by plotting $(\alpha h\nu)^2$ vs $h\nu$, based on (2) (Ray 2001)

$$\alpha h\nu = A(h\nu - E_g)^{n/2}, \quad (2)$$

where α is absorption coefficient, A a constant (independent from ν) and n the exponent that depends upon the quantum selection rules for the particular material. A straight line (figure 5) is obtained when $(\alpha h\nu)^2$ is plotted against photon energy ($h\nu$), which indicates that the absorption edge is due to a direct allowed transition ($n = 1$ for direct allowed transition). The intercept of the straight line on $h\nu$ axis corresponds to the optical band gap (E_g) and its values determined for CuO films are shown in table 3. The band gap of films which were obtained after sintering at different sintering temperatures and, thus, had different microstructures, do not differ significantly. However, the band gap values are in the expected range for CuO thin films (Oral *et al* 2004).

The current–voltage (I–V) characteristic curves of CuO films in 0·1 M NaOH (pH 13) were recorded. The curves

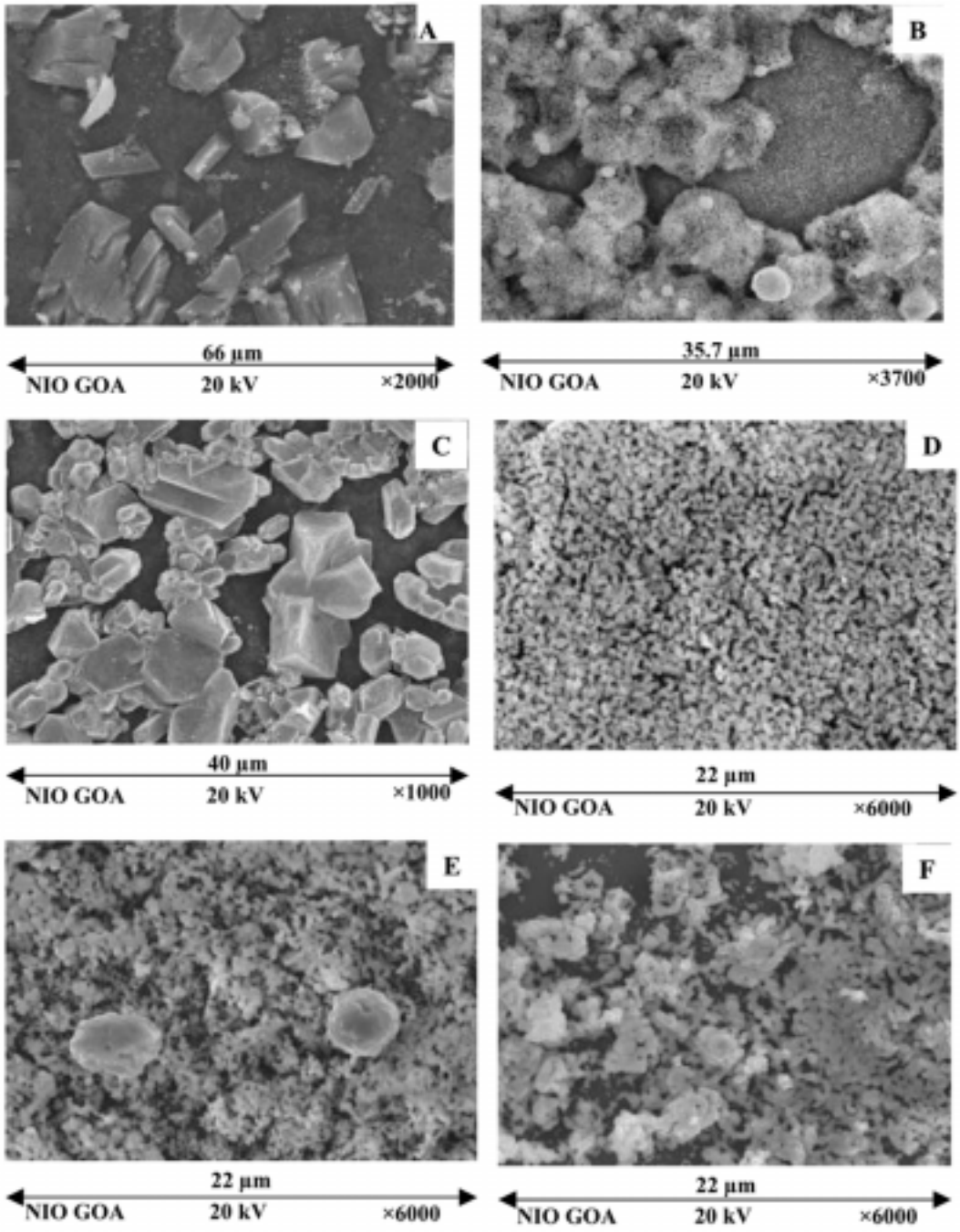

Figure 3. SEM images of ten layered copper oxide films sintered at (**A**) 400, (**B**) 450, (**C**) 500, (**D**) 550, (**E**) 600 and (F) 650°C.

demonstrated a typical feature of *p*-type semiconductor electrodes. Table 4 depicts the open circuit voltage (V_{oc}), short circuit current (J_{sc}) and fill factor (*ff*), recorded under illumination with CuO films. Figure 6 depicts the observed photocurrent density (i.e. $I_{illumination}$–$I_{darkness}$) recorded at 500 mV bias voltage with CuO films sintered at different temperatures. Since, there was no additional redox couple in the electrolyte, significant rise in photocurrent density at bias voltage, ≥ 500 mV, can be attributed to electrochemical splitting of water, which was well indicated by evolution of gases in the form of bubbles on the electrode surface. The photocurrent density increased with decrease in sintering temperature. Maximum value was recorded with films sintered at 400°C and it was nearly five-fold compared to the observed value with films sintered at 650°C. This result can be seen in terms of material properties of copper oxide phase formed. As is seen in SEM images, with rise in sintering temperature

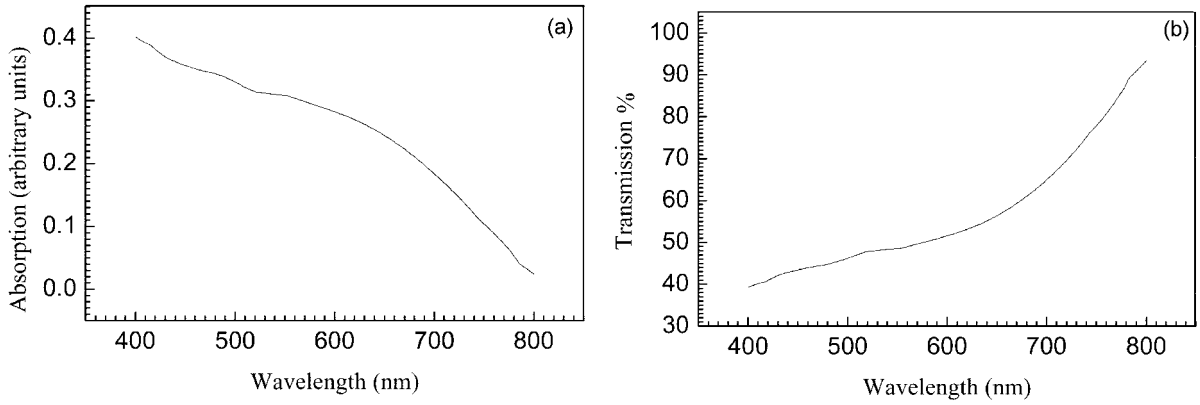

Figure 4. (**a**) Plot of absorption, and (**b**) transmission vs wavelength of twelve layered copper oxide film sintered at 450°C.

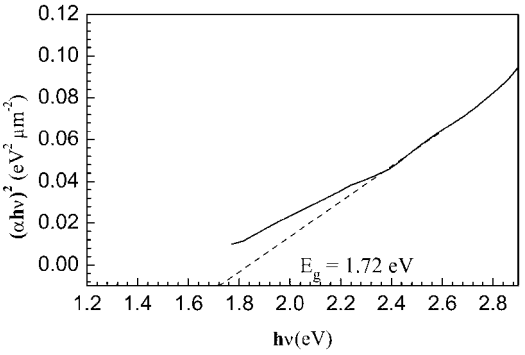

Figure 5. Plot of $(\alpha h\nu)^2$ vs $h\nu$ of twelve layered copper oxide film sintered at 450°C.

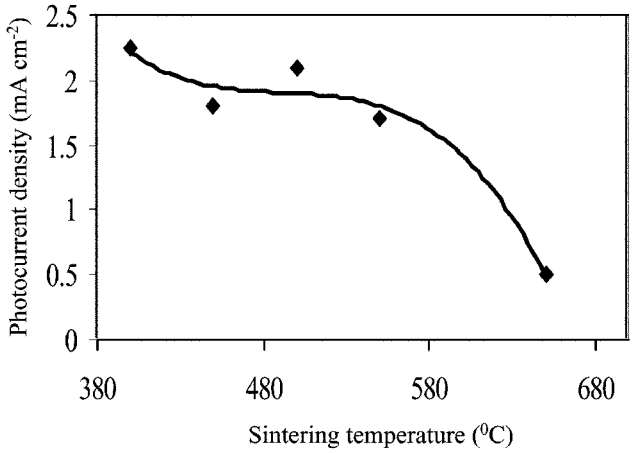

Figure 6. Photocurrent density recorded at 500 mV bias voltage with ten layered CuO film sintered at different sintering temperatures.

Table 3. Band gap energy of copper oxide films.

Sintering temperature (°C)	Number of layers	Band gap energy* (eV) Mean ± S.D.
450	6	1·76 ± 0·03
450	8	1·73 ± 0·02
450	10	1·77 ± 0·03
450	12	1·72 ± 0·03
500	10	1·79 ± 0·02
550	10	1·78 ± 0·04
600	10	1·77 ± 0·03
650	10	1·79 ± 0·04

*and S.D.: same as in table 1.

Table 4. Open circuit potential (V_{oc}), short circuit current (J_{sc}) and fill factor (ff) recorded with illumination of ten layered copper oxide film in PEC cell*.

Sintering temperature (°C)	V_{OC} (V)	J_{SC} (µA cm^{-2})	ff
400	0·68 ± 0·04	66 ± 5	0·27 ± 0·03
450	0·64 ± 0·05	86 ± 6	0·33 ± 0·03
500	0·60 ± 0·04	40 ± 5	0·22 ± 0·02
550	0·63 ± 0·06	49 ± 4	0·20 ± 0·03
650	0·70 ± 0·06	58 ± 5	0·21 ± 0·02

*and S.D.: same as in table 1.

the grain agglomerates are found to be more and more fragmented. Probably, it leads to an increase in the number of recombination centres which efficiently trap photogenerated electron–hole pairs (Yoon *et al* 2000). Additionally, the larger grain agglomerates in films sintered at lower temperatures possibly generate a lesser scattering effect that leads to a better absorption of incident photon (Yoon *et al* 1998). The observed decrease in resistance of CuO films at lower sintering temperatures might also be a cause for enhanced photoeffects. With increase in film thickness the photocurrent density decreased, which may be attributed to the increase in resistance with thickness. Further, in thicker films due to larger distances to the current collecting electrodes the transfer of photogenerated electron to electrolyte is also probably delayed (Li *et al* 1999). This will increase the chance of recombination

and, thus, may lead to the degradation of photocurrent (Yoon *et al* 1998, 2000). Although, CuO, prepared in this study, with its band gap around 1·7 eV, seems to be an efficient material for the absorption of solar energy, but, it also appears that probably its band edges are not properly aligned to redox levels corresponding to hydrogen and oxygen evolution, respectively. Hence, a definite bias voltage

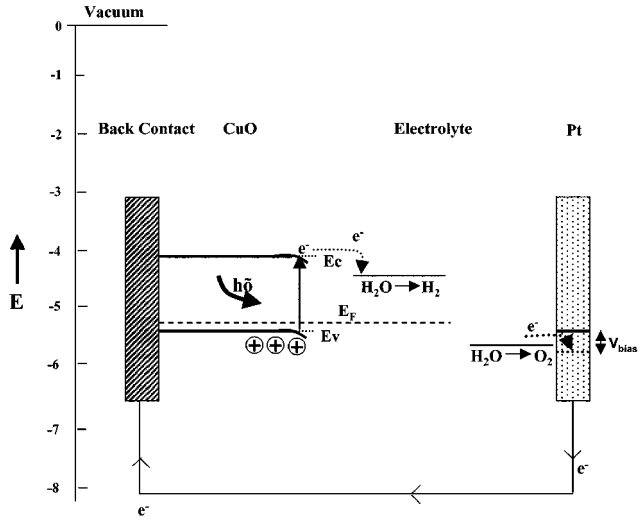

Figure 7. A tentative flow of electron in a PEC cell with CuO working electrode.

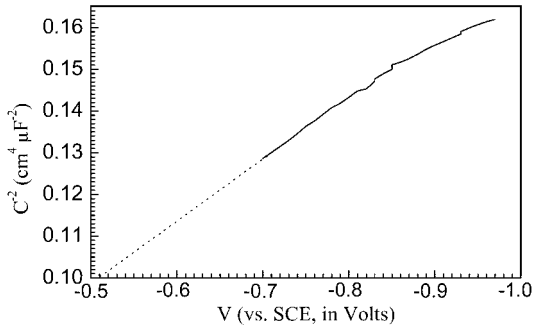

Figure 8. Mott–Schottky curve recorded with ten layered CuO film sintered at 650°C.

Table 5. Flat band potential (V_{fb}) and charge carrier density (N_D) for copper oxide films*.

Number of layers	Sintering temperature (°C)	V_{fb} (V) Mean ± S.D.	$N_D \times 10^{-24}$ (m^{-3}) Mean ± S.D.
10	400	0·59 ± 0·07	42 ± 5·9
10	450	0·47 ± 0·07	33 ± 5·3
10	500	0·22 ± 0·06	15 ± 3·6
10	550	0·20 ± 0·06	4 ± 1·3
10	600	0·24 ± 0·05	2 ± 0·6
10	650	0·21 ± 0·06	2 ± 0·8
6	450	0·35 ± 0·07	43 ± 6·7
8	450	0·45 ± 0·06	39 ± 6·0
12	450	0·39 ± 0·06	28 ± 5·1

*and S.D. : same as in table 1.

(V_{bias}) is required to allow spontaneous transfer of charge carriers across CuO–electrolyte junction. Results of the present study support this observation. Although, in this study no efforts were made to determine the exact positions of conduction and valence band edges in CuO, yet, utilizing the values reported in literature (Koffyberg and Benko 1982), a tentative flow of electrons in a PEC cell, comprising CuO and Pt as working and counter electrodes, respectively, has been depicted in figure 7. It is clear from the figure that a minimum bias voltage of around 300 mV would be needed to achieve spontaneity of electron flow. However, it should be added here that with any change in band gap or band edge positions, as a result of variations in electrolyte composition, bias voltage might also change.

Generally, the flat band potential (V_{fb}) and carrier density (N_D) are determined by measuring the capacitance (C) of the electrode/electrolyte interface at different electrode potentials (V) using (3) and (4) (Shinar and Kennedy 1982)

$$1/C^2 = [2/\varepsilon_0\varepsilon_s q N_D)][V - V_{fb} - (k_B T/q)], \quad (3)$$

$$S = 2/(\varepsilon_0\varepsilon_s q N_D), \quad (4)$$

where, ε_0 and ε_s are permittivity of free space and semiconductor electrode, respectively, q the electronic charge, T the temperature in Kelvin, k_B the Boltzmann's constant, and S the slope of $1/C^2$ vs V i.e. Mott–Schottky (MS) curve. In this study, the capacitance at CuO–NaOH junction was measured using an LCR meter (Agilent Technologies, Model: 4263B) with V varying from –1500–1500 mV, at 1 kHz signal frequency. The intercepts of the MS curves (figure 8, for films sintered at 450°C) on the potential axis are considered as the values of V_{fb} and are depicted in table 5. The observed values of V_{fb}, which are negative, and carrier density are comparable to the values reported earlier by some workers for CuO (Yoon *et al* 2000). The maximum V_{fb} was observed with films sintered at 400°C and these were the samples that yielded highest photocurrent density as well. With rise in film thickness the flat band potential decreases which is also on expected lines. The measured potentials from the intercepts of MS curves, i.e. V_{fb}, are much different from onset potentials, obtained from I^2 vs V relations and they are also 0·83–1·29 V anodic relative to $V_{fb.}$ Such a deviation indicates the presence of surface states at the electrode–electrolyte interface where carriers may recombine easily (Tafalla and Salvador 1989).

4. Conclusions

The present study, thus, leads to the following conclusions:

(I) Single phase CuO thin films with tenorite structure can be easily obtained by using preparatory method.

(II) Microstructure of the films changes on varying film preparation conditions, particularly the sintering temperature.
(III) Optical band gap of the films, measured by employing a UV-*vis* scanning spectrophotometer, lies at 1·72–1·79 eV. Hence, the films of CuO obtained by this method may be exploited as cheap and efficient solar light absorber. However, their use for PEC splitting of water is possible only with an external bias.
(IV) The films prepared at lower sintering temperature (≈ 400–500°C) yield higher photocurrent and are more efficient for photosplitting of water.
(V) Resistivity increases with thickness and thicker films are less effective in photoconversion.

Acknowledgements

Research grant received from AICTE, New Delhi (F. No. 8020/RID/R & D–118/2001-02) and UGC, New Delhi (F. No. 30-36/2004(SR)), by one of the authors (RS), is gratefully acknowledged. We are also thankful to Dr Shyam Prasad, National Institute of Oceanography, Goa and Dr R K Sharma, Solid State Physics Laboratory, New Delhi, for SEM and XRD analysis of samples.

References

Agrawal A, Chaudhary Y S, Satsangi V R, Dass S and Shrivastav R 2003 *Curr. Sci.* **85** 371
Armelao L, Barreca D, Bertappelle M, Boltaro G, Sada C and Tondello E 2003 *Thin Solid Films* **442** 48
Chandra Babu K S, Srivastava O N and Subba Rao G V 1994 *Curr. Sci.* **66** 715
Chandra N, Wheeler B L and Bard A J 1985 *J. Phys. Chem.* **89** 5037
Chaudhary Y S, Agrawal A, Shrivastav R, Satsangi V R and Dass S 2004 *Int. J. Hydrogen Energy* **29** 131
Eliseev A A, Lukashin A V, Vertegel A A, Heifets L I, Zhirov A I and Tretyakov Y D 2000 *Mater. Res. Innovat.* **3** 308
Fan F -R F and Bard A J 1980 *J. Am. Chem. Soc.* **102** 3677
Jeong Y K and Choi G M 1996 *J. Phys. Chem. Solids* **57** 81
Klug H P and Alexander L E 1974 *X-ray diffraction procedures for polycrystalline and amorphous materials* (New York: Wiley)
Koffyberg F P and Benko F A 1982 *J. Appl. Phys.* **53** 1173
Lanke U D and Vedawyas M 1999 *Nucl. Instrum. Meth. Phys. Res.* **B155** 97
Levy-Clement C, Lagoubi A, Neumann-Spullart M, Robot M and Tenne R 1991 *J. Electrochem. Soc.* **138** L69
Li J, Vizketlethy G, Revesz P and Mayer J W 1991 *J. Appl. Phys.* **69** 1020
Li Y, Hagen J, Schaffrath W, Otschik P and Haarer D 1999 *Solar Energy Mater. Solar Cells* **56** 167
Maruyama T 1998 *J. Electrochem. Soc.* **37** 4099
Morales J, Sanchez L, Martin F, Ramos-Barrado J R and Sanchez M 2005 *Thin Solid Films* **474** 133
Ohya Y, Ito S, Ban T and Takahashi Y 2000 *Key Eng. Mater.* **181** 113
Oral A Y, Mensur E, Aslan M H and Basaran E 2004 *Mater. Chem. Phys.* **83** 140
Ray S C 2001 *Solar Energy Mater. Solar Cells* **68** 307
Richthofen A, Domnic R, Cremer R and Fresenius J 1997 *J. Anal. Chem.* **358** 312
Salvador P, Guterrez C, Campet G and Hagenmuller P 1984 *J. Electrochem. Soc.* **131** 550
Shinar R and Kennedy J H 1982 *Solar Energy Mater.* **6** 323
Stilwell D E and Park S M 1982 *J. Electrochem. Soc.* **129** 1501
Tafalla D and Salvador D 1989 *J. Electroanal. Chem.* **270** 285
Yoko T, Yuasa A, Kamiga K and Sakka S 1991 *J. Electrochem. Soc.* **138** 2279
Yoon K H and Chung K S 1992 *J. Appl. Phys.* **72** 5743
Yoon K H, Shin C W and Kang D H 1998 *J. Appl. Phys.* **81** 7024
Yoon K H, Choi W J and Kang D H 2000 *Thin Solid Films* **372** 250